Thermochimica Acta 627 (2016) 9–19

Contents lists available at ScienceDirect

Thermochimica Acta

journal homepage: www.elsevier.com/locate/tca

Infrared study of the carbochlorination of MoO_3 with gaseous chlorine below 703 K

Cristina N. Guibaldo[a,*], Federico J. Pomiro[a], Georgina De Micco[a,b,**], Ana E. Bohé[a,b,c]

[a] Comisión Nacional de Energía Atómica, Av. Bustillo 9500, S.C de Bariloche, Río Negro, Argentina
[b] Consejo Nacional de Investigaciones Científicas y Técnicas, CONICET, Argentina
[c] Universidad Nacional del Comahue, Centro Regional Universitario Bariloche, Argentina

ARTICLE INFO

Article history:
Received 16 December 2015
Received in revised form 26 January 2016
Accepted 28 January 2016
Available online 22 February 2016

Keywords:
Molybdenum
Carbochlorination
FTIR
Reaction mechanism
Reaction kinetics

ABSTRACT

In this work the kinetics of the carbochlorination of molybdenum trioxide with sucrose carbon at low temperatures (below 703 K) has been studied by IR. A novel methodology for studying reaction kinetics is proposed based on on-line IR measurements of gaseous reaction products. This technique allows identification of all the species involved in the reaction system which were not taking into account in previous studies.

As predicted by thermodynamic calculations, the reaction proceeds by formation of CO_2 mainly, however formation of CO, $COCl_2$, CCl_4 and HCl also takes place. The starting temperature for the reaction is determined at about 600 K. A reaction mechanism is proposed based on the analysis of binary interactions between the reactants and their morphological changes during the reactions. The influence of carbon/oxide ratio, gaseous flow rate, sample initial mass, temperature, and chlorine partial pressure in the reaction rate was analyzed. Two kinetic regimes were identified, with activation energies of 203 ± 13 and 36 ± 6 kJ mol^{-1} which were attributed to chemical reaction control (below 653 K) and mixed reaction control at high temperatures. A reaction order of 0.5 with respect to chlorine partial pressure at 673 K was determined for the carbochlorination reaction.

1. Introduction

Molybdenum, as other refractory metals, is used in several high tech industries due to its physical and high temperature properties. To mention some examples, Mo is used in feedthrough pins of rechargeable batteries [1], furnace and glass melting components, sputtering targets for thin film manufacture [2], polymeric materials [3], among others. The wide variety of interesting properties of molybdenum alloys (electrical conductivity, high mechanical strength at high temperatures, low temperature ductility) make them useful in applications such as: glass stirrers, equipments for handling molten Zn, thermocouples, thin films in touch screen displays, furnace heating elements, lamp components, etc. [2]. Molybdenum composites materials are used mainly in semiconductors and integrated circuits [4]. Finally, molybdenum compounds such as oxides and sulphides are widely employed in catalysts in the petrochemical industry [5,6].

Chlorination and carbochlorination are used on recovery techniques of valuable metals [7,8]. Hydrometallurgical and pyrometallurgical methods have been developed for molybdenum recovery from secondary raw materials [9]. As an extractive metallurgical method, direct chlorination has been proposed for the recuperation of metals from spent catalysts. The carbon present in these raw materials could be used as a reducing agent [10]. MoO_3 chlorination with carbon, not only raises the reaction rate but also decrease the activation energy [11]. Several researchers investigated the chlorination and carbochlorination reaction of molybdenum oxide with the aim of developing efficient recovery processes that enhance metal extraction from alternative sources such as industrial waste and low-grade ores [11–13]. An amorphous carbon, such as sucrose carbon, consisting of small polycyclic aromatic carbon sheets with a high density of active sites is a promising solid for metal recovery process, synthesis and catalysis.

Chlorination and carbochlorination studies available in the literature were conducted using gravimetric and thermogravimetric techniques to obtain kinetic parameters, and possible reaction mechanisms. These studies were focused on the overall reaction through analysis of the condensed reaction products, thermodynamic calculations and mass change generated during the reaction [13–16]. The composition of gaseous phase in a carbochlorination process is complex; CO, CO_2, and $COCl_2$ gases can be formed as well

* Corresponding author.
** Corresponding author at: Comisión Nacional deEnergía Atómica, Av. Bustillo 9500, S.C de Bariloche, Río Negro, Argentina.
E-mail addresses: crisguibaldo@cab.cnea.gov.ar (C.N. Guibaldo), demiccog@cab.cnea.gov.ar (G. De Micco).

http://dx.doi.org/10.1016/j.tca.2016.01.017
0040-6031/

as metal chlorides and/or oxychlorides [17–19]. In this paper, the carbochlorination reaction of MoO_3 was studied by Fourier transform infrared spectroscopy (FTIR). This technique allows online detection of gases generated during the reaction. The reaction kinetics and mechanism can be studied according to the evolution of the gaseous phase composition.

The analysis by FTIR offers short measurement times. It can therefore be used to measure the changes over time of the gases and their concentration generated in chemical reactions [20,21].

The MoO_3 carbochlorination using black carbon was studied by Ojeda et al. [13]. In their study formation of MoO_2Cl_2 and CO_2 as reaction products was assumed, and a reaction intermediate formed by the interaction between chlorine and carbon was proposed. Our results obtained by FTIR and other complementary techniques, indicate that MoO_3 carbochlorination with sucrose carbon proceeds not only with formation of CO_2, also CO and HClO were detected.

The aim of this work is to elucidate the reaction mechanism of the MoO_3 carbochlorination at low temperatures (below 703 K), and to study its kinetics.

2. Experimental

2.1. Materials

The solids reactant were MoO_3(s) powder 99.9% (Sigma–Aldrich), $CaCO_3$ powder >99% (Sigma–Aldrich) and sucrose carbon obtained from the pyrolysis of sucrose (Fluka Chemical AG) in inert atmosphere at 980 °C during 48 h. The content of carbon in the sucrose carbon was determined by thermogravimetric calcination as 98.2%, the rest corresponds to O, H and impurities. The presence of OH groups in the sucrose carbon was identified by an IR band at 3584.5 cm^{-1}. The reactants were sieved to a size of 400 mesh (ASTM, square aperture of 37 μm). Masses of these reactants were weighed and mixed mechanically for at least 2 h to obtain different homogeneous mixtures of MoO_3-C. The composition of the mixtures, (i.e., MoO_3/C ratios) was confirmed by carbon calcination in air.

The gases used were Ar 99.99% purity (Linde), N_2 99.99% purity (Linde). and Cl_2 99.8% purity (PRAXAIR). The infrared spectra were recorded on a PerkinElmer Spectrum 400 FTIR spectrometer equipped with a DTGS detector in the range of 4000–700 cm^{-1}. The resolution was set at 2 cm^{-1}, without apodization. An IR well sealed gas cell with NaCl windows was connected after the reactor and placed in the FTIR. The optical pathway of gas cell was of 10 cm.

The gas flow was commanded by thermal mass flow controllers (Brooks 5850S) which allows working at flow rates of chlorine between 0.2 and 8 l h^{-1} and argon between 0.5 and 12 l h^{-1}.

The condensated products were characterized by scanning electron microscopy (SEM 515; Philips XL30 Electronics Instruments), X-ray diffraction (XRD, Bruker D8 Advance), with Ni filtered and Cu Kα radiation and multielement analysis was carried out by wavelength-dispersive X-ray fluorescence spectroscopy (WD-XRF, Bruker S8 Tiger).

2.2. Experimental setup

A quartz fixed bed reactor was employed to carry out the reactions; it is schematically shown in Fig. 1. This reactor consists of a horizontally mounted tube of 30 mm diameter located inside an electric furnace where the sample was introduced using a flat silica glass crucible (1 cm^2); it is connected at its entrance to a gas line. The reactor outlet is connected to a refrigerant of 50 cm long through a ground glass joint, and this to a valve system that deflect the gas to a FTIR gas cell or to a purge. The refrigerant prevents gas products, which condense at room temperature, reaching the gas

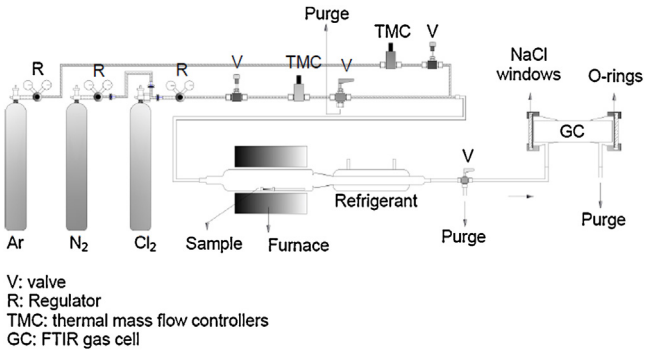

Fig. 1. Schematic diagram of the experimental set up.

cell. In non-isothermal runs, the reactant gas was introduced and the samples were heated with a linear heating rate of 5 K min^{-1}. For isothermal runs, samples were heated at the working temperature in Ar flow, before the flow was switched to reactant gas. As reaction residues, mixtures of MoO_3 and carbon were obtained, they were heated in air at 973 K for 1 h to eliminate the carbon. The new residue, consisting of unreacted MoO_3, was weighted to calculate the reaction degree.

The gas cell was specially designed to avoid formation of gastight areas in the optical pathway, this was confirmed for flows of 4 and 6 l h^{-1}. With 6 l h^{-1}, the time required to fill the cell was 10 s, this corresponds to the minimum time interval between two successive measurements of spectra to permit the release of the gas measured. The time interval between measurements was modified according to the gaseous flow used. The integrated absorbances of the peaks were measured as the area between the experimental signal and a base in the background of the spectrum.

In order to determinate the reaction starting temperature, a non-isothermal run was performed between room temperature and 823 K. The experimental conditions were: 1 atm of Cl_2 pressure, a gas flow of 6 l h^{-1}; 20 mg of initial mass (MoO_3 + C) containing 20wt. % of carbon (oxide/carbon molar ratio of 1/3). Infrared spectra were collected consecutively during the heating.

Isothermal experiments were carried out at temperatures between 613 and 703 K and chlorine partial pressure between 0.1 and 1 atm. Repeated reactions were performed under identical conditions to verify the reproducibility of the experiments.

For the identification of reaction products a heated FTIR gas cell was used that allows to perform the reaction inside the cell. The solid reactants were placed directly in the cell, the cell was purged with Ar, heated to the desired temperature and Cl_2 was injected into the cell. FTIR spectrums were recorded consecutively. This cell was not appropriated to study the reaction kinetics.

2.3. Data handling

In order to obtain the rate of a solid-gas reaction where formation of gaseous products i takes place, IR measurements of gaseous phase composition were performed during the reaction. The time of spectrum measurement (approximately 10 s) is small compared with the total time of the reaction (at least 500 s), assuming that no significant axial-mixing occurs under laminar flow condition, it can be considered that the peak areas of gaseous species are proportional to its instantaneous concentration at the time when the spectrum is measured.

Considering the Beer–Lambert law and an optical path l, the integrated absorbance A_i between the frequency range Δ of a fundamental infrared band, is defined as:

$$A_i = \int_{\Delta} \ln\left(\frac{I_0}{I}\right) d\nu = \varepsilon_i C_i l \quad (1)$$

where ε_i is the absolute integrated extinction coefficient of i, and A_i is expressed in cm^{-1}.

If the integrated absorbance vs. time curves are fitted with appropriated functions, the integral of the curves from 0 to t is proportional to the moles formed of the species i at time t, and the formation degree ζ_i at time t can be obtained from the ratio of the previous result and the value of the integral from 0 to the end of the reaction [20].

The reaction degree is defined by convenience as:

$$\zeta_i(t) = \frac{n_i(t)}{n_i(t_f)} \quad (2)$$

where $n_i(t)$ are moles of i produced from the beginning of the reaction to time t and $n_i(t_f)$ are total moles of i produced during the reaction.

Transformation degree of solid reactant x can be defined as:

$$\alpha_x(t) = \frac{m_0 - m(t)}{m_0} \quad (3)$$

where m_o is the initial mass of reactant x, and $m(t)$ is the mass of reactant x at time t. α and ζ quantities are equal if there is a unique reaction that consumes x and produces i. In general, if there are parallel reactions occurring simultaneously at the solid leading to different gaseous products, Eqs. (2) and (3) will be different.

3. Thermodynamic considerations

Molybdenum oxychloride (MoO_2Cl_2) formed in the chlorination and carbochlorination of MoO_3 was characterized in previous work [11,22]. As a first approximation, two reactions leading to formation of CO_2 and CO have negative ΔG° values, being Reaction (4) thermodynamically more feasible to occur at the temperatures studied [23]:

$$MoO_3 + Cl_2(g) + \tfrac{1}{2}C \rightarrow MoO_2Cl_2(g) + \tfrac{1}{2}CO_2(g) \quad \Delta G(\text{kJ mol}^{-1}) = -0.128T(K) - 100.1 \quad (4)$$

$$MoO_3 + Cl_2(g) + C \rightarrow MoO_2Cl_2(g) + CO(g) \quad \Delta G(\text{kJ mol}^{-1}) = -0.222T(K) - 20.56 \quad (5)$$

In the system studied the following equilibriums can be considerate:

$$CO(g) + \frac{1}{2}O_2(g) \rightarrow CO_2(g) \quad \Delta G(\text{kJ mol}^{-1}) = 0.087T(K) - 283.2 \quad (6)$$

$$CO(g) + Cl_2(g) \rightarrow COCl_2(g) \quad \Delta G(\text{kJ mol}^{-1}) = 0.135T(K) - 108.7 \quad (7)$$

$$CO_2(g) + C \rightarrow 2CO(g) \quad \Delta G(\text{kJ mol}^{-1}) = -0.177T(K) + 172.46 \quad (8)$$

A thermodynamic simulation of the MoO_3 carbochlorination was performed [23]. Fig. 2 shows the equilibrium composition (EC) as a function of temperature according to equilibrium predictions for temperatures between 300 and 750 K. The raw materials for the simulation were: solid phases: MoO_3 (four times with respect to stoichiometric $Cl_2(g)$ for Reaction (4)), and amorphous carbon in the molar ratio of 1/4 (MoO_3/C). Gaseous phase: 99.98% of Cl_2, 0.01% of HCl and 0.01% of N_2. HCl was included because sucrose carbon contains H which reacts with $Cl_2(g)$ producing HCl. It can be seen that MoO_2Cl_2, CCl_4 and CO_2 are expected to be the major gaseous products. The formation of $COCl_2$ and CO is predicted only in very small amount (below 10^{-5} molar concentration) at high temperature, and formation of HOCl and of $C_2O_2Cl_2$ would be in a molar concentration below 10^{-10}.

Kinetics and non-equilibrium conditions can influence during the carbochlorination reactions. The experimental setup used allows continuous removal of the gaseous products leading to partial pressures of these species tending to zero, whereas the partial pressure of Cl_2, which is fixed by the incoming chlorine stream, will remain constant. For this reason, the values of ΔG of reaction will be lower than the values of ΔG°, and even with a $\Delta G^\circ > 0$, a reaction could occur.

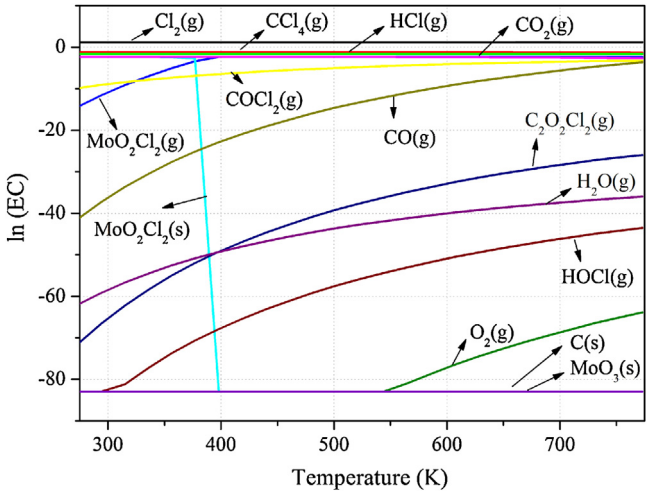

Fig. 2. Natural logarithmic of equilibrium composition (EC) as a function of temperature according to equilibrium predictions for temperatures between 300 and 750 K.

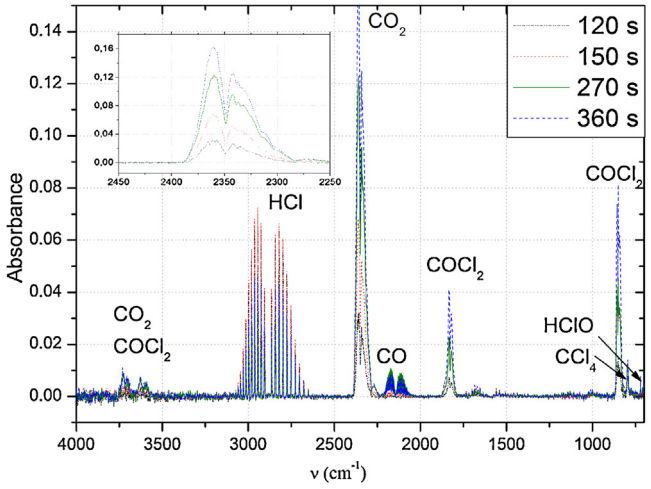

Fig. 3. Time infrared spectral evolutions in the 4000–700 cm^{-1} spectral range obtained by an isothermal reaction at 773 K. The absorption bands of reaction products are also shown.

4. Results and discussion

4.1. Identification of reaction products

Formation of MoO_2Cl_2 was determined by XRD, this reaction product is formed in gaseous state and mostly condensates in the cooler zones of the reactor and the refrigerant.

Experiment carried out on the heated gas cell at 673 K showed formation of MoO_2Cl_2, CO_2, CO, HCl and HOCl. These results are in accordance with thermodynamical predictions, where CO formation is less feasible that CO_2, but both reactions are possible. The presence of HCl and HOCl can be understood considering that the sucrose carbon contains OH (see Section 2.1).

System of Fig. 1 is employed for the kinetic study. Fig. 3 shows typical IR spectrums obtained in the chlorination reactions at

Table 1
Absorption bands of reaction products in the infrared spectrum.

Gas	IR band	Reference
CO_2	3800–3500	[24]
	2400–2280	
CO	2300–2000	[24]
$COCl_2$	3800–3400	[24,25]
	1850–1800	
	870–730	
HCl	3640–3050	[24]
	700–750	
CCl_4	810–770	[24]
HClO	730–710	[26]

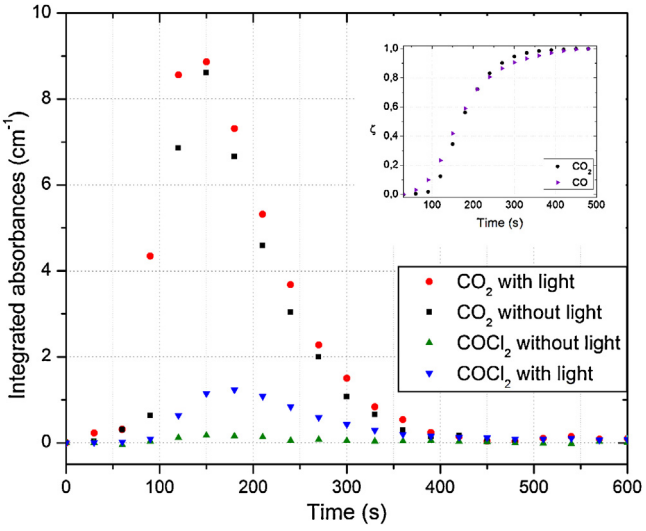

Fig. 4. CO_2 and $COCl_2$ formation in an isothermal reaction at 673 K with and without light exposure. Inset plot is the evolution of formation degree of CO_2 and CO on the reaction without light exposure.

different reaction times. In the inset of the figure, the temporal evolution of the band between 2400 and 2280 cm^{-1} corresponding to CO_2 can be observed. In Table 1, all the gaseous species detected are listed with their corresponding band. These spectrums show $COCl_2$ and CCl_4 in addition to the species detected with the heated gas cell.

Substitution reactions in the sucrose carbon can occur in a chlorine environment [14]. This was confirmed with an experiment of carbon chlorination at 673 K without molybdenum oxide where HCl, HOCl, $COCl_2$ and CCl_4 were detected, the presence of $COCl_2$ and CCl_4 suggests that some gasification of carbon does occur. However, in the experiments carried out in the heated gas cell, $COCl_2$ and CCl_4 were not detected; consequently they are being formed by reaction of other species (such as CO, HClO) in the chlorine gas flow, between the reaction zone in the reactor and the cell. The gaseous products formed in the heated gas cell are immediately evacuated due to the cell geometry, for this reason secondary products ($COCl_2$ and CCl_4) are not detected.

CO can react with Cl_2 photochemically at room temperature with formation of $COCl_2$ [27]. To verify this, experiments with and without light exposure were performed. Fig. 4 shows integrated area vs. time curves for these reactions. The curves of $COCl_2$ clearly indicate that it is a product of the photochemical reaction, because in the reaction without light a decrease in the integrated area was observed. The light does not affect CO_2 production.

HCl and HOCl are thermodynamically expected to act as chlorinating species towards MoO_3:

$$MoO_3 + 2HCl(g) \rightarrow MoO_2Cl_2(g) + H_2O(g) \quad \Delta G(\text{kJ mol}^{-1}) = -0.063T(K) + 49.8 \tag{9}$$

$$MoO_3 + 2HOCl(g) \rightarrow MoO_2Cl_2(g) + H_2O(g) + O_2(g) \quad \Delta G(\text{kJ mol}^{-1}) = -0.166T(K) + 11.5 \tag{10}$$

Thermodynamic analysis indicates that the reaction between HCl and MoO_3 is possible at 588 K without carbon. It produces MoO_2Cl_2 and H_2O. Subsequently, chlorine reacts with water to produce HCl and HClO, these species which were detected in the IR spectra, are unlikely to react again with MoO_3 because the continuous gas flow take them away from the reaction zone.

A direct chlorination of MoO_3 with HCl was performed at 673 K to corroborate the thermodynamical predictions for HCl It was found that the reaction occurs at considerable high speed. A transformation degree (α) of 0.8 was obtained after 10 min. However, due to the low H content of carbon the chlorination by HCl would be negligible. If all H contained in the carbon forms HCl and all that HCl reacts with MoO_3, the maximum transformation degree would be 0.04.

From all these measurement a rather complex reaction scenario was evidenced, which substantially differs from the usually assumed CO_2 formation. In the subsequent section quantification of CO_2 produced was performed to establish the percentage of MoO_3 that actually reacts, according to Reaction (4).

4.2. Carbon dioxide quantification in the carbochlorination reactions

The IR gas cell was in situ calibrated for CO_2 content with CO_2 generated in the complete chlorination of known amounts of $CaCO_3$ according to Reaction (11) which is thermodynamically feasible:

$$CaCO_3 + Cl_2(g) \rightarrow CaCl_2 + CO_2(g) + \tfrac{1}{2}O_2(g) \quad \Delta G(\text{kJ mol}^{-1}) = -0.112T(K) + 19.35 \tag{11}$$

The experimental conditions for these reactions were the same that for MoO_3 chlorination reactions (i.e., experimental setup of Fig. 1) 1 atm of Cl_2 pressure, gaseous flow rate of 6 l h^{-1}, heating rate of 10 K min^{-1} between room temperature and 900 K, and $CaCO_3$ initial masses from 2 to 10 mg. The IR spectra were collected every 30 s. The total moles of CO_2 produced in the reaction can be calculated from:

$$N_{CO_2} = \int_0^{t_f} C(t)_{CO_2} Q \, dt \tag{12}$$

where N_{CO_2} are moles of CO_2 in Cl_2(g), $C(t)_{CO_2}$ is the concentration of CO_2, Q is the gaseous flow rate, and the integral is over the whole reaction time. Replacing $C(t)_{CO_2}$ by Lambert–Beer law and for constant gaseous flow rate we have:

$$N_{CO_2} = \frac{Q}{\varepsilon_{CO_2} l} \int_0^{t_f} A(t)_{CO_2} \, dt \tag{13}$$

where ε_{CO_2} is the molar absorption coefficient for CO_2, l is the optical path length and $A(t)_{CO_2}$ is the measured integrated absorbance, calculated as the corresponding CO_2 peak area from the measured spectrum according to Eq. (1).The total moles of CO_2 produced in the chlorination of different quantities of $CaCO_3$ are known by the stoichiometry of Reaction (11), considering that all the carbon in $CaCO_3$ forms CO_2 (in practice this is not the exactly case, and a correction which will be explained below was made).

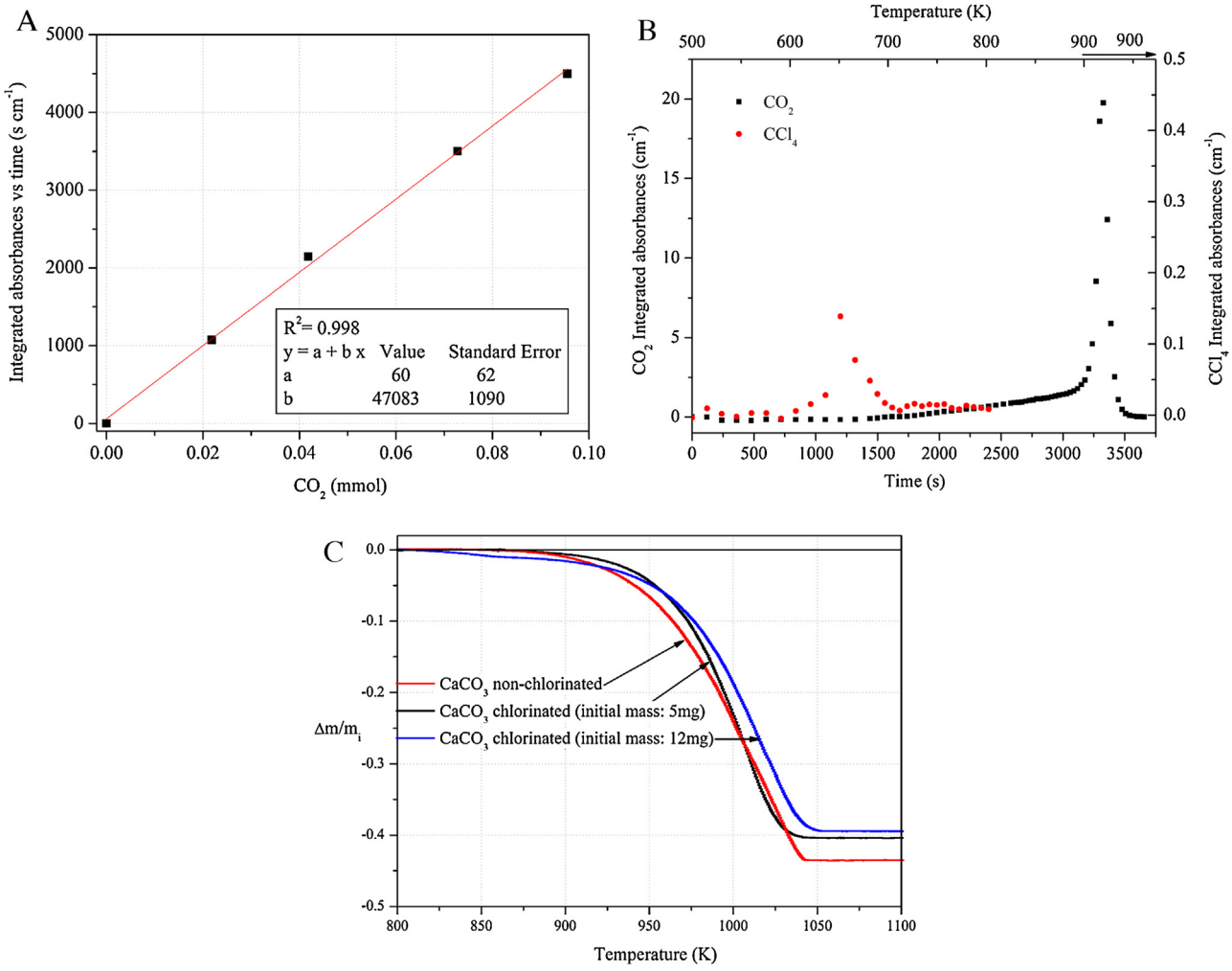

Fig. 5. (a) CO_2 quantification curve for 1 atm of Cl_2, with optic path of 10 cm and NaCl windows; (b) integrated absorbances vs. time curves of the reaction products for the $CaCO_3$ non-isothermal chlorination from 500 to 900 K (and maintained at 900 K) and (c) thermogravimetric treatment of different samples of initial and chlorinated $CaCO_3$.

From Eq. (13), a linear relation is expected when plotting the value of the integral as a function of the total moles of CO_2 for different initial masses of $CaCO_3$. The value of ε_{CO_2} can be obtained from the slope of the curve, this is shown in Fig. 5a.

A correction needs to be made due to formation of CCl_4 in the first stages of the chlorination of $CaCO_3$. This compound was detected by IR evidencing a reaction such as Eq. (14) although thermodynamically unfavorable:

$$CaCO_3 + 3Cl_2(g) \rightarrow CaCl_2 + CCl_4(g) + \tfrac{3}{2}O_2(g) \quad \Delta G(\text{kJ mol}^{-1}) = 0.029T(K) + 317.5 \qquad (14)$$

Fig. 5b shows integrated absorbances vs. time curves of the non-isothermal reaction products for the chlorination of 8 mg of $CaCO_3$. It can be seen that formation of CCl_4 occurs at temperatures below 723 K, while formation of CO_2 starts at temperatures higher than 773 K.

To determine how much sample forms CCl_4, chlorinations up to 723 K were performed. The remaining unreacted $CaCO_3$ was then treated in air by thermogravimetry using a Thermax 400 system. Fig. 5c shows the relative mass change as a function of temperature for unreacted $CaCO_3$ after chlorination up to 723 K of 5 and 10 mg of $CaCO_3$. The mass loss is due to decomposition of $CaCO_3$ leading to $CO_2(g)$ and $CaO(s)$. It was found that the amount of carbon forming CCl_4 was less than 10% of the initial $CaCO_3$, the values of N_{CO_2} were corrected with this procedure.

Table 2
Transformation degree of MoO_3 (α), and MoO_3 that reacts forming CO_2 (γ_{CO_2}) at 673 K.

α%	γ_{CO_2} %
87.4	63.6
85.7	70.7
85.5	70.9
88.5	61.4
90.0	60.7
85.9	58.6
84.5	74.6
85.9	58.6
89.6	63.4

With these results, the $CO_2(g)$ generated during the carbochlorination reactions through Reaction (4) can be calculated with Eq. (13). In Table 2 the amount to MoO_3 that reacts forming CO_2 γ_{CO_2} at 673 K are presented. It can be seen that the average value is 65% with a standard deviation of 6%.

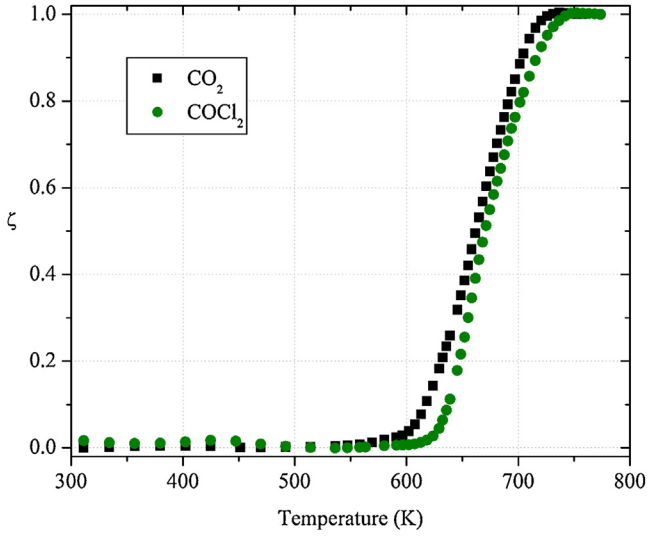

Fig. 6. Degree of product formation in non-isothermal reaction of MoO_3 carbochlorination from room temperature to 773 K.

4.3. Reaction mechanism and kinetics

4.3.1. Non-isothermal carbochlorination: initial temperature

Non-isothermal carbochlorination of MoO_3 is shown in Fig. 6 where the reaction degree for CO_2 and $COCl_2$ as a function of temperature are presented. It can be noticed that the reaction starts at approximately 600 K with formation of CO_2(g) and at 625 K with formation of CO(g), the later is evidenced by the presence of $COCl_2$(g) which is the reaction product of CO(g) and Cl_2(g) as discusses earlier.

4.3.2. Isothermal carbochlorinations and effect of carbon content

Isothermal reactions were performed for temperatures between 613 K and 673 K, it was observed that the reactions were not complete, even CO_2 and $COCl_2$ IR signal were not detected at the end of the experiments, unreacted MoO_3 oxide and carbon remained in the crucible. Fig. 7a shows the transformation degree obtained at different temperatures. It can be seen that it increases as temperature rises being the maximum value $\alpha = 0.85 \pm 0.04$ for 673 K. At this temperature, after 500 s the gaseous product IR signals disappear, a reaction of 1000 s was performed to corroborate that the reaction does not continue. Similar transformation degree was obtained taking into account the experimental scattering.

The influence of carbon content was analyzed with different oxide/carbon ratios. The experimental results (Fig. 7b) show an increase in the rate of CO_2 formation as carbon content increases until 1/4 molar relation. The difference observed for 1/5 and 1/4 molar relation is within the range of the experimental scatter. It was not observed difference in the transformation degree of MoO_3; the α for these reactions at 673 K was 0.87 ± 0.02.

Two hypotheses were considered to understand this behavior (i.e., the incompleteness of the chlorination reactions): (a) product condensation at the reaction surface (b) the increasing distance between reactive solids due to its consumption during the reaction, which prevents the reaction to proceed [28]. The former was discarded because not MoO_2Cl_2 was detected with the reaction residue even interrupting the reaction sharply to avoid its volatilization, and due to the high vapor pressure of MoO_2Cl_2 it is not expected to be formed as a condensate. On the other hand, a reaction in which the solids were place unmixed in the crucible lead to no reaction indicating that the distance between the solids affects the reaction. To understand the reaction mechanism, the interactions between carbon and chlorine as well as chlorinated carbon and molybdenum oxide were studied.

4.3.3. Carbon/chlorine interaction

Sucrose carbon was chlorinated at 673 K. The gaseous products detected by IR were: HCl and CCl_4. A mass increase of 3.4wt% of the initial mass was obtained after the reaction. WD-XRF analysis of the solid residue indicated that the chlorinated sample contains 4.5wt% of chlorine.

The infrared spectrum of the chlorinated sucrose carbon shows a band on 720.52 cm^{-1}, which correspond to stretching vibration of C—Cl bond. Similarly, Papirer et al. [29] observed C—Cl bonds on carbon black chlorinated at 723 K. They are formed essentially by addition or hydrogen substitution processes [14].

Fig. 8 shows SEM images of sucrose carbon before (a and b) and after (c and d) the chlorination at 673 K. These micrographs show an average particle size of 10–50 μm for initial carbon which has completely smooth surfaces and morphological changes were not observed after the chlorination evidencing that not substantial attack of carbon takes place.

4.3.4. Chlorinated carbon/MoO_3 interaction

To determine if chlorination reaction occurs between chlorine chemisorbed in sucrose carbon and MoO_3 (in absence of chlorine gas) a reaction was performed in which the chlorinated carbon was mixed with molybdenum oxide and the mixture (80.2wt% of carbon) was placed in the reactor of Fig. 1 (without refrigerant) and purged with Ar. The furnace was heated to 673 K once the furnace has reached that temperature the reactor was slide into the furnace and IR measurements were recorded consecutively. MoO_2Cl_2, CO and CO_2 were detected evidencing that the reaction occurs between the solids. The transformation degree of 0.08 was obtained.

4.3.5. Chlorine/carbon/MoO_3 interaction

Fig. 9 shows the morphology of MoO_3 and carbon after a carbochlorination reaction. In Fig. 9a, the particles of MoO_3 (light) and carbon (dark) can be distinguished. The carbon particles are not substantially attacked as also shown in Fig. 9b. Fig. 9c shows an oxide particle that has several concavities in which two small pieces of carbon can be observed. This is evidencing that the reaction took place locally at those concavities between the oxide and carbon, leading to consumption of both reactants due to formation of gaseous MoO_2Cl_2, CO and CO_2. Finally in Fig. 9d a carbon particle can be seen, it has many holes at its surface, evidencing that the particle has been severally attacked during the reaction.

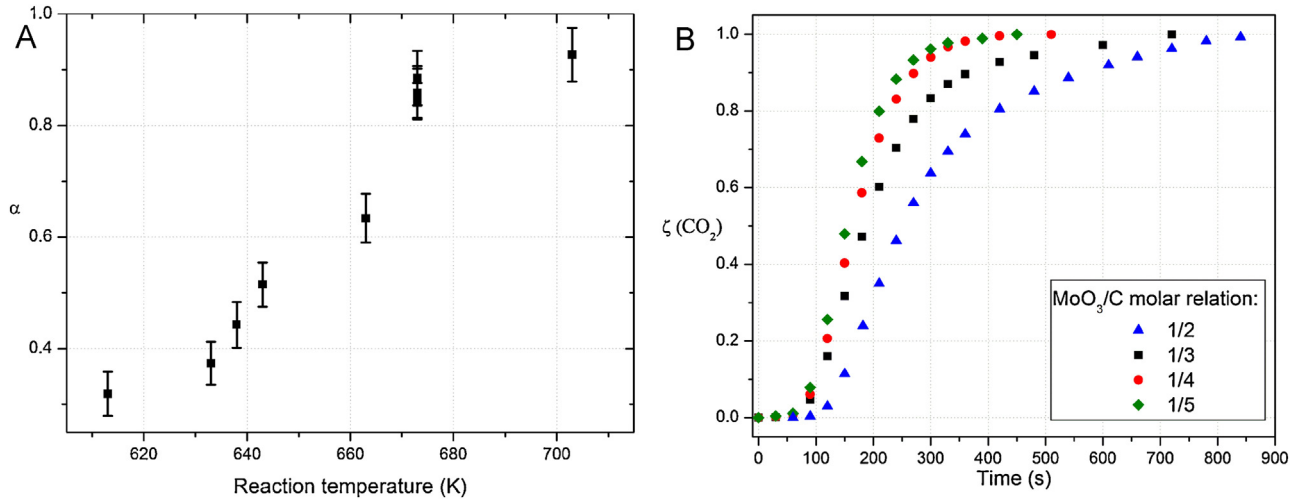

Fig. 7. (a) Effect of reaction temperature in the MoO_3 transformation degree; and (b) effect of carbon content in the rate of CO_2 formation in isothermal reactions at 673 K.

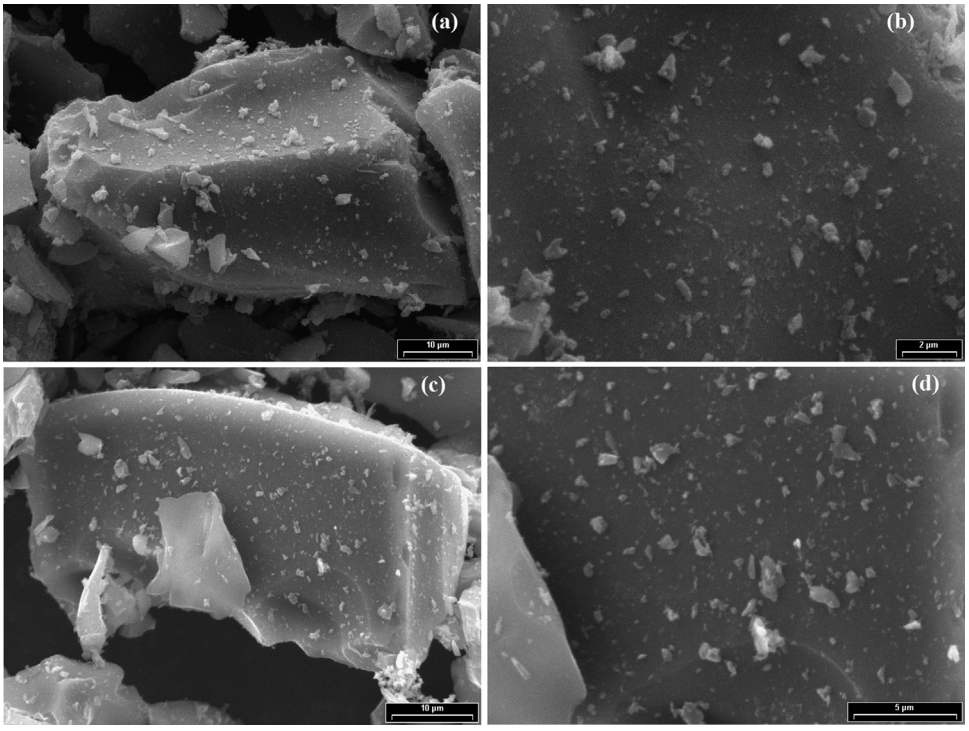

Fig. 8. SEM images of sucrose carbon: (a, b) before and (c, d) after treatment with Cl_2 at 673 K.

4.3.6. Reaction mechanism

Two main possible reaction mechanisms were proposed in the literature for carbochlorination reactions at high temperatures (above 733 K): (a) a two stages behavior where the first stage (fast, not temperature dependent) proceeds through formation of intermediate species such as Cl radical at the active sites of carbon which subsequently react with the oxide leading to formation to O_2 that reacts with carbon to produce CO and CO_2, and a second stage (slow) where carbon active sites are exhausted and oxidation of carbon with O_2 leads to an atmosphere of reduced oxygen potential that enhances chlorination of the oxide [28,30], and (b) formation of an activated C–MO_x–Cl complex at the MO_x/C/Cl_2 interface which is subsequently decomposed into products [31].

In the first step of the mechanism proposed by Pasquevich and Amorebieta [30], which corresponds to formation of Cl radical by the reaction of Cl_2 with C, the reaction rate was independent of temperature, being gaseous diffusion of Cl_2 in the boundary layer the rate determining process. The reaction rates of the carbochlorination studied here are not independent of temperature (below 653 K), and the reaction rate is three orders slower than the rate of gaseous diffusion (see Section 4.3.2) this could indicate that the radical formation does not occur at the low temperatures studied, or, if radical formation does take place, the rate is determined by a different process which is influenced by temperature such as dissociation of Cl_2 molecule at the carbon surface.

Regarding the second stage of the mechanism proposed by Pasquevich and Amorebieta [30] that involves carbon oxidation by O_2, it is not expected to proceed to a large extent because oxidation of sucrose carbon by molecular oxygen in chlorine atmosphere starts at 833 K [32]. This temperature is higher than the temperatures studied here; formation of CO and CO_2 in the first part of the chlorination curves may be due to the reaction of a more reactive

oxygen species such as oxygen radical. After about 500 s the reactions tend to stop, this is attributed to the exhaustion of carbon active sites; further oxidation of carbon with O_2 is extremely slow at these temperatures.

Taking into consideration the results obtained, the mechanism proposed for the system under study is as follows:

- Formation of Cl—C bonds over C surface

$$Cl_2(g) + H - C* \rightarrow Cl - C* - HCl(g) \quad (15)$$

$$Cl_2(g) + C = C* \rightarrow ClC* - C*Cl \quad (16)$$

The symbol C^* denotes a surface carbon atom (active site).

- Chlorination at the C/MoO_3 interface

$$MoO_3 + 2Cl - C* \rightarrow MoO_2Cl_2(g) + 2C + O^{\bullet} \quad (17)$$

- Carbon oxidation

$$C + 2O \rightarrow CO_2(g) \quad (18)$$

$$C + O^{\bullet} \rightarrow CO(g) \quad (19)$$

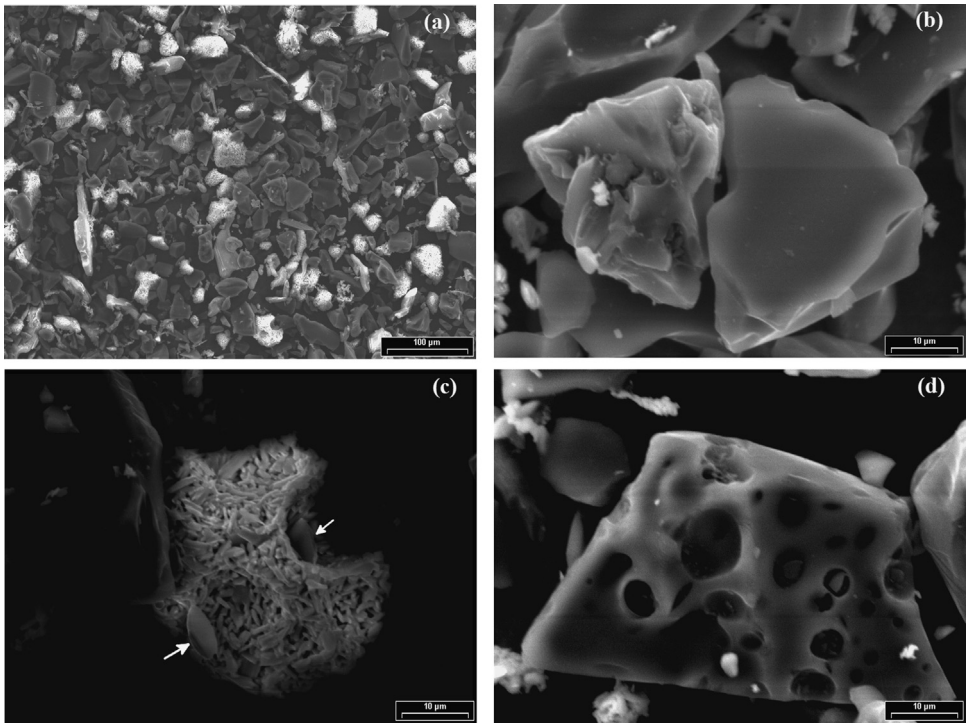

Fig. 9. SEM images of solid reside after MoO_3 carbochlorination reaction at 673 K.

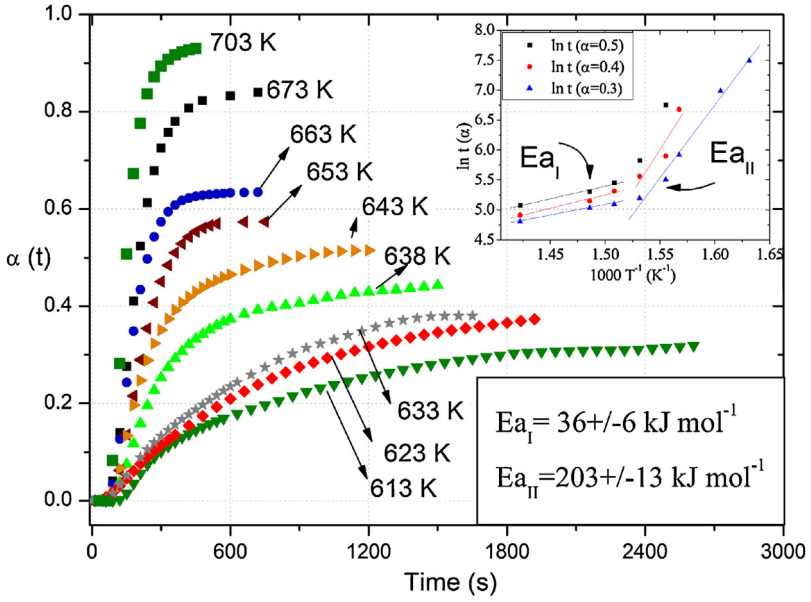

Fig. 10. MoO_3 transformation degree as a function of time at different temperatures obtained by Eq. 26. Inset plot shows two kinetic regimes and the estimation activation energy of each.

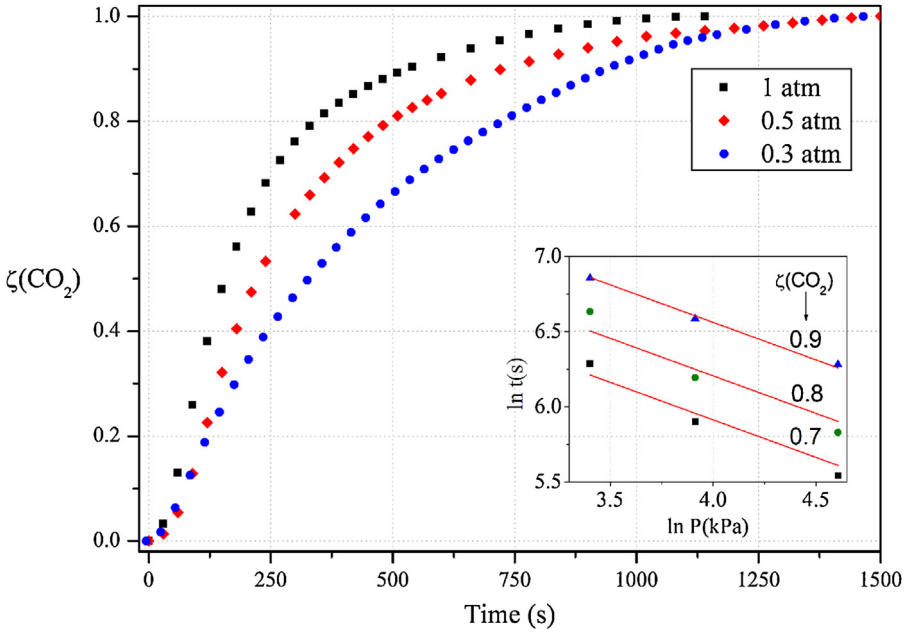

Fig. 11. Effect of Cl_2 partial pressure in the CO_2 formation rate in MoO_3 carchlorination reaction at 703 K. Plot shows the estimation of reaction order with respect to chlorine partial pressure.

This mechanism suggests the formation of an activated MoO_3–ClC intermediary between the surfaces of carbon (on C—Cl bond) and of oxide, which decomposes into oxychloride and active oxygen atom. Similarly to that proposed by Yang and Hlavacek [31] on the TiO_2 carbochlorination.

4.3.7. Reaction kinetics

To determine the reaction intrinsic parameters, the reaction rate has to be measured in the chemical kinetic regime (i.e., in absence of mass transfer processes affecting the reaction rate). The effect of gaseous flow rate and sample mass were evaluated. It was obtained that for gaseous flow rate above 6 l h^{-1} and masses between 10 and 30 mg no mass transport phenomena affect the reaction rate (the details of the experiments are in Appendix).

The experimental reaction rate in moles of Cl_2 reacting per unit time and unit area N_{Cl_2} was compared with the theoretical calculated rate of chlorine diffusion through the boundary layer above the sample plate according to Fickís Law. The rate of diffusion can be estimated by [33]:

$$N_{Cl_2} = -\frac{D}{RT\delta}\left(p_{Cl_2,s} - p_{Cl_2,b}\right) \tag{20}$$

The value of D was calculated for a CO_2—Cl_2 mixture according to the Chapman–Enskog correlation [34] and corresponding temperature, $p_{Cl_2,s}$ was calculated assuming equilibrium at the reaction surface, and δ was estimated as the boundary layer thickness using Von-Kármání's analysis [35]. The obtained value for N_{Cl_2} was in the order of 10^{-2} moles of Cl_2 s^{-1} m^{-2} for temperature between 573 and 703 K.

The experimental values of N_{Cl_2} were calculated, using to CO_2 quantification curve, from the experimental results from the steeper slope (r) of the Cl_2 mol vs. time curves corresponding to the carbochlorination reactions at different temperatures. Considering the reaction surface as the sample projected area A, we have:

$$N_{Cl_2,exp} = \frac{r}{A} \tag{21}$$

The values obtained are in the order of 10^{-5} moles of Cl_2 s^{-1} m^{-2}. It can be concluded that the mass transfer controlled rate would be significantly faster, and the rates measured correspond to the chemical process.

4.4. Effect of temperature. Estimation of activation energy

As discussed earlier, the results (Fig. 7a) show that the MoO_3 transformation degree rises as temperature increases. The degree of reaction curves for CO and CO_2 were obtained of the FTIR measurements. These curves are equal (see inset Fig. 4) for all the temperatures studied. From these data, and considering that MoO_3 reacts through Eqs. (4) and (5), we have:

$$\alpha_{MoO_3}(t) = \alpha_{MoO_3}(t)_{byEq.(4)} + \alpha_{MoO_3}(t)_{byEq.(5)} \tag{22}$$

where:

$$\alpha_{MoO_3}(t)_{byEq.(4)} = \frac{n_{CO_2}(t)}{n_{CO_2,Totals}} \times \frac{n_{MoO_3,Eq.(4)}}{n_{MoO_3,initial}} = \zeta_{CO_2}(t) \times \alpha_{MoO_3,byEq.(4)} \tag{23}$$

$$\alpha_{MoO_3}(t)_{byEq.(5)} = \frac{n_{CO}(t)}{n_{CO,Totals}} \times \frac{n_{MoO_3,Eq.(5)}}{n_{MoO_3,initial}} = \zeta_{CO}(t) \times \alpha_{MoO_3,byEq.(5)} \tag{24}$$

where $\alpha_{MoO_3}(t)_{byEq.x}$ is the transformation degree of MoO_3 due to reaction of Eq. x, and $n_{MoO_3,Eq.x}$are the moles of MoO_3 consumed by reaction of Eq. x.Replacing:

$$\alpha_{MoO_3}(t) = \zeta_{CO_2}(t) \times \alpha_{MoO_3,by\ Eq.(4)} + \zeta_{CO}(t) \times \alpha_{MoO_3,byEq.(5)} \tag{25}$$

Since ζ of CO_2 and CO are equal and $\alpha_{MoO_3,byEq.(4)} + \alpha_{MoO_3,by\ Eq.(5)} = \alpha_{MoO_3,final}$, the curves of MoO_3 transformation degree, can been calculated as:

$$\alpha_{MoO_3}(t) = \alpha_{MoO_3,final} \times \zeta_{CO_2}(t) \tag{26}$$

The corresponding curves are shown in Fig. 10. It can be seen that the plots show a deceleratory behavior, i.e., reaction rate decreases with reaction progress, and the deceleration occurs faster

as the temperature decreases. As discussed in Section 4.3.6, this was attributed to the fast reaction involving Cl radical or/and intermediate complex between carbon and oxide, followed by a very slow reaction due to carbon oxidation which due to the low temperatures employed is extremely slow and the reaction almost stops after exhaustion of the active sites.

The activation energy was calculated from the slope of the $\ln t(\alpha)$ vs. T^{-1} (inset of Fig. 10) according to Flynn method (for details of calculation procedure see Ref. [17]). Two different kinetic regimes can be distinguished: for the lower temperatures (below 653 K) an activation energy of 203 ± 13 kJ mol^{-1} was calculated which corresponds to chemical control because no gaseous flow or mass effects were observed (see Section 6) and the experimental rate of reaction is three orders higher than the rate of gaseous diffusion (see Section 4.3.7). For the higher temperatures, above 653 K, the low activation energy of 36 ± 6 kJ mol^{-1}, indicates that a mixed control of reaction rate is taking place.

The activated energy calculated could correspond to the intermediary formation, or dissociation of Cl_2 at the reaction surface.

4.5. Effect of Cl_2 partial pressure

Experiments were carried out to determinate the reaction order with respect to Cl_2 partial pressure. We proposed a power dependency $p_{Cl_2}^m$ for chlorine partial pressure. The procedure applied to obtain m is detailed elsewhere [19].

Fig. 11 shows the degree of CO_2 formation vs. time curves for different Cl_2 partial pressures at 703 K. From the natural logarithm of time for different formation degrees as a function of natural logarithm of P_{Cl_2}, a reaction order m (Fig. 11 inset shows these plots) of 0.5 was determined.

A maximum value of α of 0.5 ± 0.02 was obtained for all pressures studied, indicating that it was not affected by Cl_2 partial pressure.

5. Conclusions

The results of the MoO_3 chlorination in presence of sucrose carbon studied by FTIR allow the following conclusions:

- The proposed methodology using on-line FTIR yields reproducible and representative results of the gaseous phase of the reaction system. The MoO_3–C–Cl_2(g) system was analyzed by this methodology.
- The interpretation of the FTIR measurements showed that both CO(g) and CO_2(g) are formed during the carbochlorination reaction. This behavior differs from the assumption made in previous works.
- The initial reaction temperature is approximately 600 K with formation of CO_2(g) and 625 K with formation of CO(g).
- Several gaseous species were detected: CO_2, CO, $COCl_2$, CCl_4, HClO and HCl. Being $COCl_2$ and CCl_4 not direct reaction products, but formed between gaseous species after the reaction.
- Rates of CO_2 and CO formation are equal, which suggest that the reaction intermediate is the same for both reaction products.
- The reaction rate is controlled by intrinsic particle kinetics between 623 K and 653 K. Under these conditions, the activation energy of about 203 ± 13 kJ mol^{-1} was obtained. The reaction order with respect to chlorine partial pressure was of 0.5 at 673 K.
- A reaction mechanism is proposed in which an intermediate would be formed, which could be chlorine radical or an activated complex between chlorinated carbon and oxide.

Acknowledgements

The authors would like to thank the Consejo Nacional de Investigaciones Científicas y Técnicas (CONICET) and Agencia Nacional de Promoción Científica y Tecnológica (ANPCyT PICT-2012-2475) for financially supporting this work.

Appendix.

To determinate the experimental conditions under which the reaction rate is not dependent by mass transfer processes, it was carried out experiments at 673 K with a molar relation of 1/4 (MoO_3/C) and a Cl_2 pressure of 1 atm.

The gaseous flow rate was analyzed between 4 and 6 l h^{-1}. It can be seen that the effect of the gaseous flow rate on reaction rate was negligible beyond 6 l h^{-1} (Fig. A1).

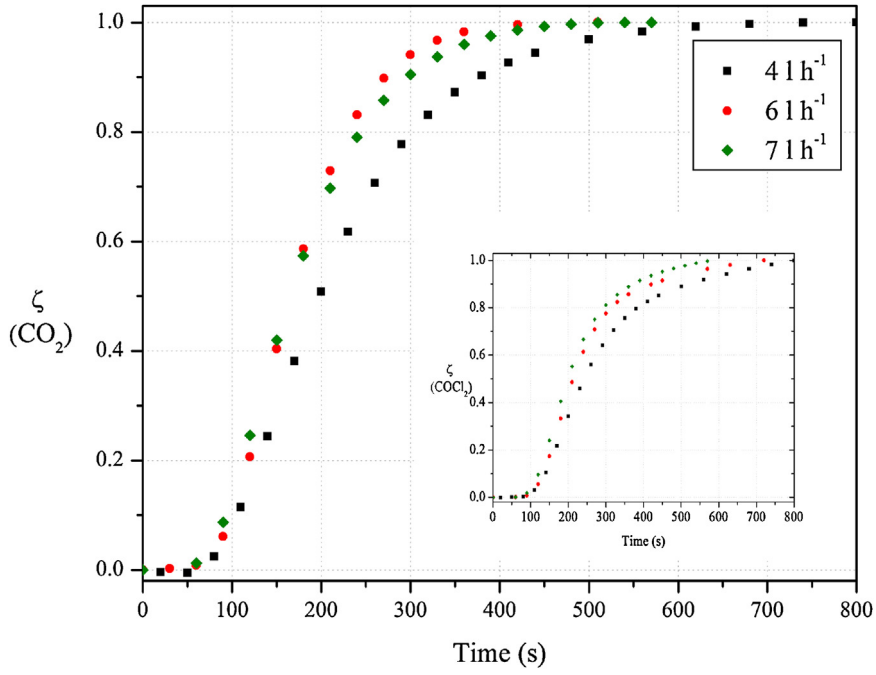

Fig. A1. Influence of gaseous flow in the CO_2 formation during the isothermal reactions at 673 K. Inset plot is the effect of gaseous flow in the $COCl_2$ formation.

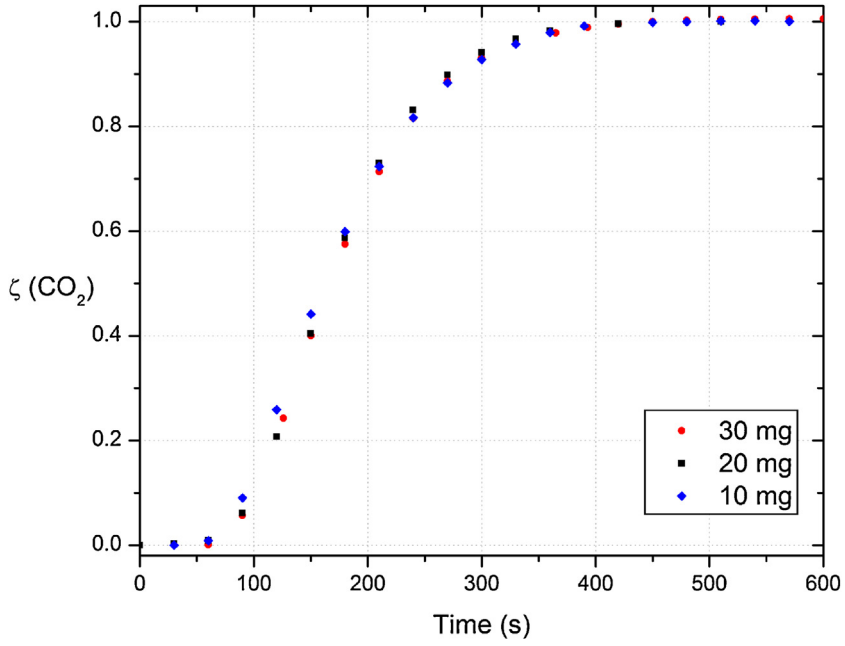

Fig. A2. Influence of initial sample mass in the CO_2 formation during the carbochlorination reactions at 673 K.

Fig. A2 shows the curve for the reaction with different initial sample masses. It was observed that the initial mass is not influencing the kinetics parameters.

References

[1] J. Lin, G. Jiang, Pulsed Nd.YAG Laser Fine Spot Welding for Attachment of Refractory Mini-pins, SPIE Digital Library, 2013, pp. 8608.
[2] J.A. Shields, Applications of Molybdenum Metals and Its Alloys, International Molybdenum Association, London, UK, 2013.
[3] A.G. Kholmogorov, V.V. Kryuchkov, Synthesis, Properties and Application of Novel Polymeric Materials, Niitekhim, Moscow, Russia, 1983.
[4] A.K. Vasudévan, J.J. Petrovic, A comparative overview of molybdenum disilicide composites, Mater. Sci. Eng. A 155 (1–2) (1992) 1–17.
[5] R.R. Schrock, A.H. Hoveyda, Molybdenum and tungsten imido alfylidene complexes as efficient olefin-methatesis catalysts, Olefin Metathesis Catal. 42 (2003) 4592–4633.
[6] G. Murali Dhar, B.N. Srinivas, M.S. Rana, Manoj Kumar, S.K. Maity, Mixed oxide supported hydrodesulfurization catalysts—a review, Catal. Today 86 (2003) 45–60.
[7] C.-H. Kim, S.I. Woo, S.H. Jeon, Recovery of platinum-group metals from recycled automotive catalytic converters by carbochlorination, Ind. Eng. Chem. Res. 39 (5) (2000) 1185–1192.
[8] Y. Mochizuky, N. Tsubouchi, K. Sugawara, Selective recovery of rare earth elements from Dy containing NdFeB magnets by chlorination, Sustain. Chem. Eng. 1 (2013) 655–662.
[9] A.G. Kholmogorov, O.N. Kononova, G.L. Pashkov, S.V. Kachin, O.N. Panchenko, O.P. Kalyakina, Review—molybdenum recovery from mineral raw materials by hydrometallurgical methods, Eur. J. Min. Process. Environ. Prot. 2 (2) (2002) 82–93, 1303–0868.
[10] L. Zeng, C.Y. Cheng, A literature review of the recovery of molybdenum and vanadium from spend hydrodesulphurization catalysts. Part I: metallurgical processes, Hydrometallurgy 98 (2009) 1–9.
[11] M.E. Djona, I. Allain Gaballah, Kinetic of chlorination and carbochlorination of molybdenum trioxide, Metall. Mater. Trans. 26B (1995) 703–710.
[12] G. De Micco, M. Carignan, C.A. Canavesio, A.E. Bohé, Determination of intrinsic parameters for MoO_3 chlorination with Cl_2 gas between 798 and 873 K, Thermochim. Acta 543 (2012) 211–217.
[13] M.W. Ojeda, J.B. Rivarola, O.D. Quiroga, Study on chlorination of molybdenum trioxide mixed with carbon black, Minerals Eng. 15 (2002) 585–591.
[14] J.A. González, J.B. Rivarola, M.C. del Ruiz, Kinetics of chlorination of tantalum pentoxide in mixture with sucrose carbon by chlorine gas, Metall. Mater. Trans. 35B (2004) 439–448.
[15] A. Movahedian, Sh. Raygan, M. Pourabdoli, The chlorination kinetics of zirconium dioxide mixed with carbon black, Thermochim. Acta 512 (2011) 93–97.
[16] S. Sarkar, P. Kr. Das, Non-isothermal oxidation kinetics of single- and multi-walled carbon nanotubes up to 1273 K in ambient, J. Thermal Anal. Calorim. 107 (2012) 1093–1103.
[17] J.P. Gaviría, A.E. Bohé, Carbochlorination of yttrium oxide, Thermochim. acta 509 (2010) 100–110.
[18] L. Niu, T. Zhang, P. Ni, G. Lü, K. Ouyang, Fluidized-bed chlorination thermodynamics and kinetics of Kenya natural rutile ore, Trans. Nonferrous Met. Soc. China 23 (2013) 3448–3455.
[19] F.J. Pomiro, G.G. Fouga, J.P. Gaviría, A.E. Bohé, Study of the reaction stages and kinetics of the europium oxide carbochlorination, Metall. Mater. Trans. B 46 (1) (2014) 304–315.
[20] I. Mincu, M. Hillebrand, A. Allouche, M. Cossu, P. Verlaque, J.P. Aycard, J. Pourcin, Photolysis of the dichlorocyclobutenedione in rare gas at 10 K. Infrared spectral analysis and ab initio calculations of vibrational frequencies. First identification of two new species (dichloro-substituted bisketene and dichloropropadienone). Kinetics and reaction mechanism, J. Phys. Chem. 100 (40) (1996) 16045–16052.
[21] B.-S. Chiou, S.A. Khan, Real-Time FTIR and in situ rheological studies on the UV curing kinetics of thiol-ene polymers, Macromolecules 30 (1997) 7322–7328.
[22] A. Guethert, R. Muenze, B. Eichler, Contribution to the thermodynamics of the molybdenum-oxygen-chlorine system, J. Radioanal. Chem. 62 (1–2) (1981) 91–101.
[23] H.S.C. 6. 12, Chemistry for Windows, Outkumpu Research Oy, Pori, Finland, 2007.
[24] NIST Standard Reference Data, Free database.
[25] I, A. Mincu, M. Allouche, Cossu, J. Aycard, FT-IR identification, characterization and ab initio vibrational analysis of phosgene, oxalyl chloride and 1,2-dichlorocyclobutene-3,4-dione trapped in argon cryogenic matrices, Spectrochim. Acta 51A (3) (1995) 349–362.
[26] A.I. Karelin, Z.I. Grigorovich, V. Ya. Rosolovskii, Vibrational spectra of perchloric acid-I. Gaseous and liquid $HClO_4$ and $DClO_4$, Spectrochimica Acta 31A (1975) 765–775.
[27] H. Schnöckel, R.A. Eberlein, H.S. Plitt, Infrared spectra of matrix isolated ClCO and ab initio calculation, J. Chem. Phys. 97 (4) (1992) 4–7.
[28] I. Barin, W. Schuler, On the kinetics of the chlorination of titanium dioxide in the presence of solid carbon, Metall. Trans. B 11 (1980) 199–207.
[29] E. Papirer, R. Lacroix, J.-B. Donnet, G. Nansé, P. Fioux, XPS studyof the halogenation of carbon black. Part 2. Chlorination, Carbon 33 (1) (1995) 63–72.
[30] D.M. Pasquevich, V.T. Amorebieta, Mass spectrometric study of volatile products during the carbochlorination of zirconia, Phys. Chem. 96 (4) (1992) 530–533.
[31] F. Yang, V. Hlavacek, Carbochlorination kinetics of titanium dioxide with carbon and carbon monoxide as reductant, Metall. Mater. Trans. B 29B (1998) 1297–1307.
[32] J.A. González, M.C. del Ruiz, A. Bohé, D. Pasquevich, Oxidation of carbán in the presence of chlorine, Carbon 37 (1999) 1979–1988.
[33] J. Szekely, J.W. Evans, H.Y. Sohn, Gas–solid reaction, 1976 (Chapter 2–3), pp. 10–22, 66–73.
[34] J.O. Hirschfelder, C.F. Curtiss, R.B. Bird, Molecular theory of gases and liquids, 1956.
[35] F.M. White, Fluid Mecanics, 7th ed., 2011 (Chapter 7), 461–470.